Calculations of Inelastic Scattering of Neutrons by Heavy Nuclei*

E. H. AUERBACH AND S. O. MOORE
Brookhaven National Laboratory, Upton, New York
(Received 15 April 1964)

Neutron-scattering cross-section data between 0.1 and 3.0 MeV for U, Th, Bi, Pb, Au, W, and Ta have been fitted using a local, spherical, spin-dependent optical potential with a minimum number of parameters. Total cross sections and differential elastic angular distributions, corrected to include compound elastic scattering, are used. With the "entrance-channel" parameters thus determined, the Hauser-Feshbach statistical model gives reasonable predictions of the cross sections for inelastic scattering of neutrons by U^{238}, Th^{232}, Bi^{209}, Pb^{208}, Au^{197}, W^{184}, and Ta^{181}. The latitude in fitting entrance-channel data allowed by the optical-model parameters is sufficient to mask effects arising from nonlocality, deformation, and width distributions. To a very high degree, this relatively simple model is shown to be adequate for the presently available data.

I. INTRODUCTION

FOR over a decade, since the early work of Feshbach, Porter, and Weisskopf (FPW),[1] calculations of total neutron scattering have been performed using complex potential models of varying degrees of complexity. The inability of the FPW model to calculate directly the compound elastic contribution to elastic scattering resulted in some difficulty in the energy range up to a few MeV because there that contribution could not be neglected. The abandonment of the square well in favor of a diffuse-edged one[2] and the addition of the neutron's spin-orbit interaction[3] to the potential led to an increase in the number of parameters describing the optical potential. This did result in adequate calculations[4,5] at those energies where simple assumptions regarding the compound elastic contribution were acceptable. More recently, the energy dependence of the optical-potential parameters has been eliminated by use of a nonlocal potential.[6] The calculations of Bjorklund and Fernbach[4] and of Perey and Buck[6] give good reproduction of neutron cross sections over a large range of elements and energies with relatively simple optical potentials.

Hauser and Feshbach,[7] following suggestions by Wolfenstein,[8] described a method for calculating inelastic scattering through the compound-nucleus mechanism based on simple statistical assumptions concerning the behavior of compound-nucleus processes. The compound elastic-scattering contributions are also obtainable by this method. Crucial to the use of this theory is the calculation of transmission coefficients. Straightforward schemes, proceeding from a complex potential model for scattering have been used widely with varying degrees of success. Recently, more sophisticated schemes for calculating transmission coefficients have been employed.[9,10]

Significant improvement in experimental technique ever the last few years has made available a considerable quantity of inelastic scattering data of higher accuracy. This makes possible a more precise analysis of that data in terms of the Hauser-Feshbach theory. We have taken a representative sample of isotopes of heavy nuclei and fit the scattering data, total and elastic, in the energy range 0.1 to 3.0 MeV on an element by element basis. The parameters thus determined were used to calculate inelastic scattering and compared to the data. The optical model and Hauser-Feshbach model used are described briefly in Sec. II. The data, level schemes, and calculations for the heavy nuclei U^{238}, Th^{232}, Bi^{209}, Pb^{208}, Au^{197}, W^{184}, and Ta^{181} are discussed in Sec. III. General features of the calculated cross sections are considered in Sec. IV.

II. THEORY

The heavy-element region between tantalum and uranium includes deformed nuclei. Thus one would not expect, *a priori*, to be able to fit the experimental data assuming a spherical optical potential. The calculations presented here are based on the assumption of a local spherical optical potential; agreement or disagreement between calculated and experimental results then indicates how sensitive optical-model fitting is to this simplification.

Calculations of the optical potential, whether proceeding from two-body data or from more refined models of the behavior of nuclear matter, predict a variation of the opical-model parameters with the energy of the incident particle. The work of Perey and Buck,[6] proceeding from phenomenological considerations, fits neutron scattering data over a range of energies with a nonenergy-dependent but nonlocal optical potential. Examination of the equivalent local parameters indi-

* This work performed under the auspices of the U. S. Atomic Energy Commission.

[1] H. Feshbach, C. E. Porter, and V. F. Weisskopf, Phys. Rev. **96**, 448 (1954).
[2] R. W. Woods and D. S. Saxon, Phys. Rev. **95**, 577 (L) (1954).
[3] S. Fernbach, W. Heckrotte, and J. V. Lepore, Phys. Rev. **97**, 1059 (1955).
[4] F. Bjorklund and S. Fernbach, Phys. Rev. **109**, 1295 (1958).
[5] J. R. Beyster, R. G. Schrandt, M. Walt, and E. Salmi, Los Alamos Laboratory Report LA-2099, 1957 (unpublished).
[6] B. Buck and F. Perey, Nucl. Phys. **32**, 353 (1962).
[7] W. Hauser and H. Feshbach, Phys. Rev. **87**, 366 (1952).
[8] L. Wolfenstein, Phys. Rev. **82**, 690 (1951).
[9] P. A. Moldauer, Phys. Rev. **123**, 968 (1961); **129**, 754 (1963).
[10] G. R. Satchler, Phys. Letters **7**, 55 (1963).

TABLE I. Compound elastic corrections to differential elastic scattering of 1.0 MeV neutrons by U^{238} and Bi^{209}.[a,b]

Angle (deg)	U^{238} $d\sigma_{se}$	U^{238} $d\sigma_{ce}$	U^{238} $d\sigma_{el}$	Bi^{209} $d\sigma_{se}$	Bi^{209} $d\sigma_{ce}$	Bi^{209} $d\sigma_{el}$
0	2.02	0.061	2.08	1.12	0.136	1.26
30	1.17	0.046	1.21	0.709	0.126	0.835
60	0.216	0.029	0.245	0.208	0.114	0.322
90	0.201	0.022	0.224	0.228	0.109	0.337
120	0.214	0.029	0.244	0.223	0.114	0.337
150	0.057	0.046	0.103	0.059	0.126	0.185
180	0.006	0.062	0.068	0.034	0.136	0.170

[a] All cross sections are in b/sr.
[b] se, ce, and el refer to shape elastic, compound elastic, and elastic, respectively (Ref. 1).

cates the presence of energy dependence when viewed in this (local) way. The energy range we consider is relatively small; accordingly, we use a local, nonenergy-dependent optical potential. The resulting parameters may then be considered to be the average local equivalent parameters over this range, when viewed in terms of a nonlocal potential model.

Total cross sections can be calculated using the optical model directly. In the case of elastic scattering, the (one-channel) optical model does not include the contribution due to compound elastic scattering—formation of a compound nucleus followed by decay of the compound nucleus through the entrance channel. The Hauser-Feshbach statistical model,[7] which we use to calculate inelastic-scattering cross sections, also gives the compound elastic corrections. Table I illustrates the value of calculated compound elastic contributions for two of the isotopes of this study. The compound elastic contributions are neither isotropic nor small.

These two models, linked together, form the basis of our calculations.

A. Optical Model

We employ a conventional, local optical model which includes the neutron's spin-orbit interaction. The optical potential takes the form

$$V(r)=-V_{RE}f(r)-iV_{IM}g(r)-V_{SR}h(r)\mathbf{l}\cdot\boldsymbol{\sigma}, \quad (2.1)$$

where the real nonspin-dependent part has a Saxon form[2]

$$f(r)=\frac{1}{1+\exp[(r-R)/a]}, \quad (2.2)$$

the imaginary part has a Gaussian form

$$g(r)=\exp[-(r-R)^2/b^2], \quad (2.3)$$

and the spin-dependent part is real and of the Thomas form[3]

$$h(r)=\left(\frac{\hbar}{\mu_\pi c}\right)^2\frac{1}{r}\left|\frac{df(r)}{dr}\right|. \quad (2.4)$$

The radii R are related to the mass A and size parameter R_0 by the relation $R=R_0A^{1/3}$. In all, (2.1)—(2.4) involve six parameters: three strengths, V_{RE}, V_{IM}, V_{SR}, and three lengths, R(or R_0), a, and b.

Imaginary parts of the form

$$\frac{d}{dr}\left[\frac{1}{1+\exp[(r-R)/a']}\right] \quad (2.5)$$

have been used. The significant features of the imaginary part, that it be surface peaked and have some width, are the same for both (2.3) and (2.5); the two forms differ nontrivially only for large values of $|r-R|$. Since no appreciable physical effect of this difference at the energies we consider has been suggested, we have used the older Gaussian form. For a wide range of widths b and depths V_{IM}, there exist equivalent pairs (b,V_{IM}) which give substantially the same results—larger V_{IM}'s correspond to smaller b's and vice versa. Thus we have arbitrarily fixed $b=1.0$ F and let the variation during searches occur on V_{IM} alone. Both the results of Bjorklund and Fernbach[4] ($b=0.98$ F) and of Perey and Buck[6] ($a'=0.47$ F, the equivalent $b\approx 2a'$) are consistent with our choice for b.

The solution of the Schrödinger equation with complex potential given by (2.1) yields phase shifts $\delta_{lj}(E)$ from which one can calculate total and differential elastic-scattering cross sections (the latter uncorrected for compound elastic contributions). In addition, transmission coefficients

$$T_{lj}(E)=1-|\eta_{lj}(E)|^2, \quad (2.6)$$

where $\eta_{lj}(E)=e^{2i\delta_{lj}(E)}$, are obtained. These are necessary for the inelastic scattering calculations which follow.

B. Hauser-Feshbach Statistical Model

The Hauser-Feshbach model[7] is based on the statistical assumption that all states of the compound nucleus which are accessible on the basis of conservation of energy, angular momentum, and parity do participate, but that formation and decay take place in an incoherent manner. A consequence of this is that all angular distributions of scattered particles are symmetric about 90°. The extent to which this is satisfied by the data is a measure of the validity of the assumption.

Hauser and Feshbach[7] assumed that the probability of decay of the compound nucleus yielding a neutron of given orbital angular momentum l is a function of the transmission coefficient $T_l(E)$ which does not depend on the total angular momentum j of the outgoing neutron nor on the spin of the target nucleus. The total cross section for the scattering of neutrons of incident energy E by a nucleus with a ground state having spin I_0 and parity Π_0, to produce outgoing neutrons of energy E' leaving the residual nucleus in a state with

energy E_q having spin I_q and parity Π_q is given by

$$\sigma(E,E')=\frac{\pi\lambda\!\!\!^{-2}}{2(2I_0+1)}\sum_l T_l(E) \times\sum_J \frac{\epsilon_{jlJ}(2J+1)\sum_{l'j'}\epsilon_{j'l'J}T_{l'}(E')}{\sum_{p,l'',j''}\epsilon_{j''l''J}T_{l''}(E_p')}, \quad (2.7)$$

where the sum over p in the denominator is taken over all accessible levels $E_p<E$, including the ground-state $E_0(E_p'=E-E_p)$; the l' and l'' sums run over all values which lead to final states consistent with parity conservation

$$(-1)^{l'}\Pi_q=(-1)^l\Pi_0, \quad (-1)^{l''}\Pi_p=(-1)^l\Pi_0;$$

the j's are the channel spins and take on values $j_{1,2}=I_0\pm\frac{1}{2}$, $j_{1,2}'=I_q\pm\frac{1}{2}$ and $j_{1,2}''=I_p\pm\frac{1}{2}$;

$$\epsilon_{jlJ}=\left\{\begin{matrix}2 \text{ if both } j_1 \text{ and } j_2\\ 1 \text{ only one of } j_1 \text{ and } j_2\\ 0 \text{ neither } j_1 \text{ nor } j_2\end{matrix}\right\} \text{satisfy } |J-l|\le j_i \le (J+l);$$

and J takes on all values consistent with conservation of angular momentum in the formation of the compound nucleus

$$|l-j_i|\le J\le(l+j_i).$$

The angular distribution has the form

$$\sigma(E,E',\theta)=\frac{\lambda\!\!\!^{-2}}{4}\frac{1}{2(2I_0+1)}\sum_l T_l(E) \times\sum_J \frac{\epsilon_{jlJ}\sum_{l',j'}\epsilon_{j'l'J}T_{l'}(E_q')}{\sum_{p,l'',j''}\epsilon_{j''l''J}T_{l''}(E_p')} \times\sum_{L\text{ even}}|Z(lJlJ;jL)Z(l'Jl'J;j'L)P_L(\cos\theta)|, \quad (2.8)$$

where all sums preceding the last factor are taken in the same manner as for (2.7); the final sum is over even L for $L\le\min(2l,2l',2J)$; and $Z(abcd;ef)$ are the Z coefficients of Blatt and Biedenharn.[11]

More recently, extensive calculation with spin-dependent optical potentials has shown the existence of wide differences in transmission coefficients for the two total angular momenta of a neutron corresponding to the same orbital angular momentum.[12] In what follows, we discard the channel spin notation and use j to denote the total angular momentum of the neutron. We shall use transmission coefficients $T_{lj}(E)$ and modify (2.7) and (2.8) accordingly[13]:

$$\sigma(E,E')=\frac{\pi\lambda\!\!\!^{-2}}{2(2I_0+1)}\sum_{j,l}T_{lj}(E) \times\sum_J\frac{(2J+1)\sum_{j'l'}T_{l'j'}(E')}{\sum_{p,j'',l''}T_{l''j''}(E_p')}, \quad (2.9)$$

$$\sigma(E,E',\theta)=\frac{\lambda\!\!\!^{-2}}{4}\frac{1}{2(2I_0+1)}\sum_{j,l}T_{lj}(E) \times\sum_J\frac{(2J+1)^2\sum_{j'l'}T_{l'j'}(E')}{\sum_{p,j''l''}T_{l''j''}(E_p')} \times\sum_{L\text{ even}}(-1)^{I-I'}Z(l'j'l'j';\tfrac{1}{2}L)Z(ljlj;\tfrac{1}{2}L) \times W(Jj'Jj';I'L)W(JjJj;IL)P_L(\cos\theta). \quad (2.10)$$

Here J,j',j'' satisfy the relations

$$|I_0-j|\le J\le(I_0+j),$$
$$|J-I_q|\le j'\le(J+I_q),$$
$$|J-I_p|\le j''\le(J+I_p),$$

l's satisfy the relations $l=j\pm\frac{1}{2}$ (similarly for l' and l''), and

$$(-1)^{l'}\Pi_q=(-1)^l\Pi_0,$$
$$(-1)^{l''}\Pi_p=(-1)^l\Pi_0.$$

The apparently different structure of these equations is due to the abandonment of the channel spin notation in favor of one which considers the total neutron angular momentum. This is more convenient because the transmission coefficient now depends on the neutron's total angular momentum as well as its orbital angular momentum.

Compound elastic-scattering contributions are obtained by letting $E'=E$, $I_q=I_0$, and $\Pi_q=\Pi_0$ in Eqs. (2.9) and (2.10).

III. CALCULATIONS

For each of the isotopes considered, we chose a set of total cross-section data for the energy range to be fit and sets of differential elastic angular distributions at energies well distributed throughout that range. These constituted the "entrance channel" data used. The choice for angular distributions was sometimes limited by unavailability of data. Where more than one set of data was available, the choice was dictated by considerations of date of the experiment, errors assigned

[11] J. M. Blatt and L. C. Biedenharn, Rev. Mod. Phys. 24, 258 (1952).

[12] E. H. Auerbach and F. G. J. Perey, Brookhaven National Laboratory Report BNL-765 (unpublished).

[13] L. C. Biedenharn, *Angular Correlations in Nuclear Spectroscopy*, edited by F. Ajzenberg-Selove (Academic Press Inc., New York, 1960), Part B, Chap. V.C.

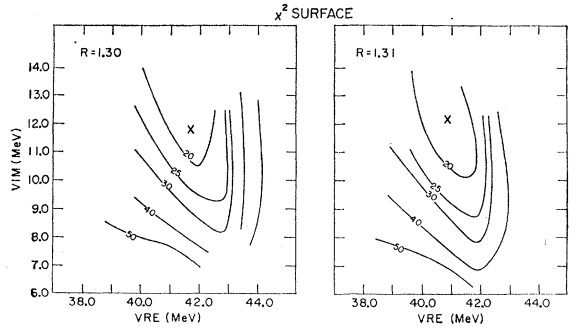

FIG. 1. χ^2 surfaces in the vicinity of the minimum for entrance channel data for U^{238}. The minima, denoted ×, have a χ^2 value of 17. The value of a is 0.49 F. Note that a reduction of V_{IM} from 12.0 to 8.0 MeV increases χ^2 only from 17 to 30. The scale is such that a χ^2 value of 28 is equivalent to an rms deviation of one standard deviation in the data.

by the authors, and consistency between experiments. Detailed discussion for specific isotopes is given below.

As a measure of the fit of a calculated set of cross sections to the experimental data, we used

$$\chi^2 \equiv \chi^2_{\text{tot}} + \chi^2_{\text{ang dist}}, \tag{3.1}$$

where

$$\chi^2_{\text{tot}} = \sum_k \left(\frac{\sigma(E_k)^{\text{calc}} - \sigma(E_k)^{\text{expt}}}{\Delta\sigma(E_k)^{\text{expt}}} \right)^2 \tag{3.2}$$

and

$$\chi^2_{\text{ang dist}} = \sum_k \left[\frac{1}{N_k} \sum_n \left(\frac{d\sigma(E_k,\theta_n)^{\text{calc}} - d\sigma(E_k,\theta_n)^{\text{expt}}}{\Delta\sigma(E_k,\theta_n)^{\text{expt}}} \right)^2 \right]; \tag{3.3}$$

$\sigma(E_k)$ and $\Delta\sigma(E_k)$ are the total cross sections and errors in total cross sections at energy E_k, $d\sigma(E_k,\theta_n)$ and $\Delta\sigma(E_k,\theta_n)$ are the differential elastic cross sections and respective errors at energy E_k and center-of-mass angle θ_n. The factor $1/N_k$ (N_k is the number of angles θ_n at which the data are given for the energy E_k) ensures that each angular distribution has weight determined by the error assignments and not by the number of points in the angular distribution.

First, the values of χ^2 were calculated for a coarse grid in the five-dimensional parameter space (V_{RE}, V_{IM},V_{SR},R,a) using only optical-model cross sections (not corrected for compound elastic scattering). This gave a general picture of the parameter space and indicated the region(s) in which a minimum was expected. In general, within the range of values of these five parameters usually accepted in optical-model calculations, the minima are unique in this "gross" sense. There did exist, however, directions or hyperplanes in the 5-dimensional space along which moderate changes in the parameters produced changes in χ^2 which were not appreciable. A typical set of χ^2 contours (the case illustrated is for U^{238}) is in Fig. 1. Along a line in the $V_{RE}-V_{IM}$ plane χ^2 differences are not significant. Consequently, a choice of "best parameters" on this basis is somewhat arbitrary.

The coarse grid search was then followed by a multidimensional search to find the minimum regions in the parameter space. Then, with compound elastic-scattering corrections included, the minimum search was repeated. The resulting minima were in different regions in parameter space but not far removed from the minima for the uncorrected cross sections. As an additional check, the surrounding neighborhood in parameter space was examined to determine tolerance limits on the parameters found and to guard against false minima.

The choice of level schemes is discussed in detail under each isotope separately.

Inelastic scattering data usually presented no questions of choice. More recent work has significantly smaller errors than previous work. Fitting is done considering only the later work. Some earlier cases are shown and are quite consistent.

Using the parameters which defined χ^2 minima for entrance channel data, we then calculated the inelastic-scattering cross sections. The results were generally in agreement as to shape, but not necessarily as to scale or position along the energy axis. If we define a measure of the fit of calculated inelastic-scattering cross sections to an excited level E_j by

$$\chi_j^2 = \sum_k \left(\frac{\sigma(E_k)^{\text{calc}} - \sigma(E_k)^{\text{expt}}}{\Delta\sigma_k{}^{\text{expt}}} \right)^2, \tag{3.4}$$

in analogy with (3.2), and the total χ^2 for all excited levels by

$$\chi^2_{\text{inel}} = \sum_j \chi_j^2, \tag{3.5}$$

we can search for a minimum χ^2_{inel} in the optical-model parameter space. When a good fit was obtained, it was generally not far removed from the minimum defined by the entrance channel data. In particular, the minimum region with respect to χ^2_{inel} overlaps the minimum region for the entrance channel χ^2. When this occurs, as is the case for all isotopes we considered except W^{184} and Au^{197}, the same set of parameters fits both entrance channel and inelastic-scattering data. Detailed discussion appropriate to particular isotopes is given below.

All calculations were done with the computer program, ABACUS-2 (slightly modified, to facilitate rapid handling of the entrance channel data over a range of energies only some of which had differential elastic-scattering data), which performs optical-model and Hauser-Feshbach calculations in one package. The parameter space scan and χ^2-minimum search features of the program were extremely useful in this study. This program has been used widely in the last two years, establishing our confidence in its substantial accuracy.

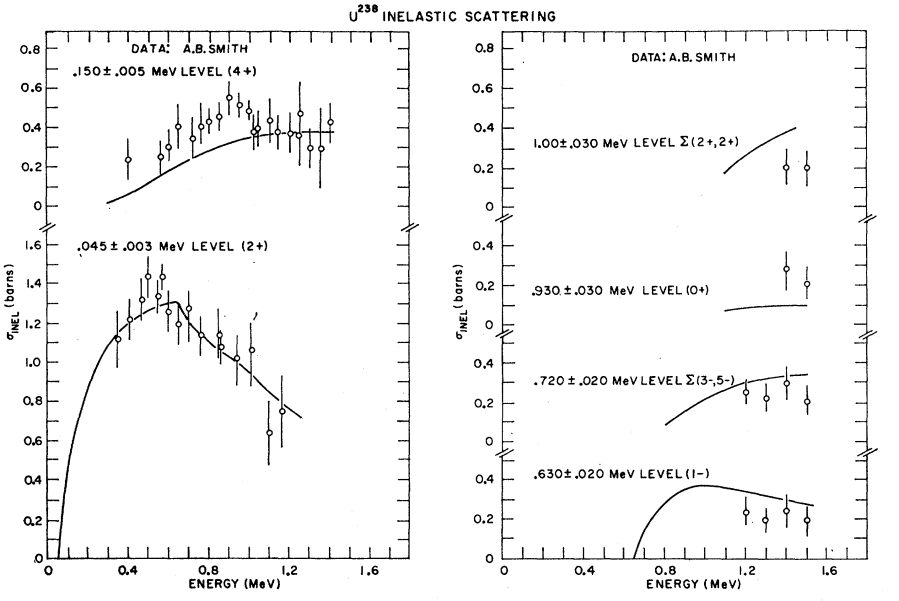

FIG. 2. Calculated values for inelastic scattering of neutrons by U^{238} using the Hauser-Feshbach theory and the optical-model parameters determined by fitting the entrance channel data. Energy captions are those measured by Smith for the data shown; calculated values are for the levels of the scheme of Fig. 3.

U-238

Total neutron cross sections for uranium from 0.1 to 2.0 MeV are taken from BNL-325[14]; these are consistent data due to two groups.[15] We assumed total errors of 5%. In view of the smooth variation with energy of the calculated results, the averaging over 100-keV intervals by the authors introduces no difficulties for our calculations.

Differential elastic-scattering cross-section data at energies of 0.35, 0.415, 0.475, 0.57, 0.60, 0.65, 0.72, 0.77, 0.95, 1.10, 1.17, and 1.25 MeV, as well as the inelastic scattering data are the work of Smith[16] who used pulsed-beam fast time-of-flight techniques. For the angular distribution data, we assumed 10% errors; for the inelastic-scattering data the errors indicated by the author (see Fig. 2) were used.

Several level schemes have been considered for U^{238}. Elbek, Igo, Stephens, and Diamond[17] proposed one, based on Coulomb excitation of U^{238} by O^{16}, which differs from the one we finally used in the neighborhood of 700 keV, where they have only 1^- and 3^- levels, and in the energy assignments above 900 keV. Cranberg[18] suggested another which is based on a study of the γ rays of U^{238} by Lind and Day; this scheme is sparse above 900 keV. Dresner[19] proposed a level scheme which uses levels above 900 keV in analogy to the level scheme of Pu^{238}; the levels in the vicinity of 700 keV are somewhat different. In all of these the first rotational states (2^+, 4^+, and 6^+) are at the same energies. Differences occur in the positions of the 1^- and 3^- octupole vibration levels near 700 keV and in the higher levels above 900 keV. Interchanging level schemes had no great qualitative effect on the inelastic scattering cross sec-

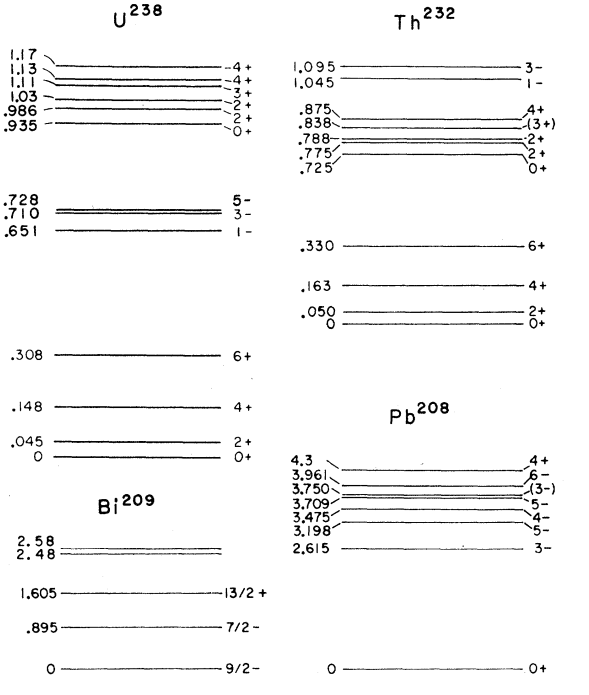

FIG. 3. Level schemes for U^{238}, Th^{232}, Bi^{209}, and Pb^{208}. For the choice of individual assignments, see text Sec. III.

[14] D. J. Hughes and R. B. Schwartz, *Neutron Cross Sections*, (U. S. Government Printing Office, Washington, 1958), 2nd ed.
[15] H. H. Barschall, R. K. Adair, C. K. Bockelman, X. Graves, R. L. Henkel, and R. E. Peterson, Los Alamos Report LA-1060, 1950 (unpublished); R. L. Henkel, L. Cranberg, G. A. Jarvis, R. Nobles, and J. E. Perry, Jr., Phys. Rev. **94**, 141 (1954).
[16] A. B. Smith, Nucl. Phys. **47**, 633 (1963).
[17] B. Elbek, G. Igo, F. Stephens, Jr., and R. M. Diamond, Lawrence Radiation Laboratory Report UCRL-9566, 1960 (unpublished).
[18] L. Cranberg, Argonne National Laboratory Report ANL-6122, 1959 (unpublished).
[19] L. Dresner, Nucl. Sci. Eng. **10**, 142 (1961).

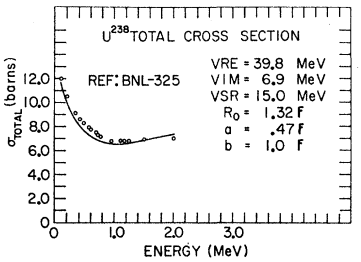

FIG. 4. Experimental and calculated (solid line) total neutron cross sections of U. The data are from Refs. 14 and 15. The calculated values are within the 5% errors assigned the data.

tions for the first two excited states, the ones for which the best data are available.

Recently, Smith[16] obtained the cross sections for the inelastic excitation of residual nuclear levels at 0.045 $\pm$0.003, 0.150$\pm$0.005, 0.630$\pm$0.020, 0.720$\pm$0.020, 0.930 $\pm$0.030, 1.00$\pm$0.03, and 1.05$\pm$0.03 MeV. Because of his experimental verification, we settled upon the level scheme given in Fig. 3. The 0^+, 2^+, 4^+, 6^+ rotational states are common to all proposals. The middle section (700-keV vicinity) is based on the Cranberg study of Lind and Day's work; 0.654 MeV is almost within the error quoted by Smith for 0.630 MeV; the 3^- and 5^- levels correspond to Smith's 0.720-MeV level. The higher levels (above 900 keV) are a composite of the other two schemes; energy assignments were chosen to fall within the errors of Smith's data. Spins and parities are consistent with the systematics but there are probably some levels in this region which have been missed.

In fitting the entrance channel data a minimum region of high real potential depth was found (V_{RE} = 65.0 MeV, V_{IM} = 13.5 MeV, V_{SR} = 5.0 MeV, R_0 = 1.30 F, a = 0.44 F, b = 1.0 F) in addition to the more conventional set. We discarded this solution in accord with shell-model considerations. A set of "best parameters" located in the minimum regions for both entrance channel and inelastic scattering data is: V_{RE} = 39.8 MeV, V_{IM} = 6.9 MeV, V_{SR} = 15.0 MeV, R_0 = 1.32 F, a = 0.47 F, b = 1.0 F. Figures 4 and 5 compare the calculated total and differential elastic cross sections with experimental data. Agreement for total cross sections is quite good. In the case of the angular distributions agreement is good at lower energies; at higher energies, the small disagreement may be attributed to the inclusion of the first inelastic group with the elastic component in the experimental data. In Fig. 2, the calculated inelastic-scattering cross sections are compared to the experimental data. Agreement for the 2^+ level (0.045 MeV) is excellent; the 4^+ level (0.150 MeV) is good though a little low; calculated results for the 6^+ level (0.308 MeV) do not exceed 0.03 b at 1 MeV and are not shown. The experimental values for inelastic-scattering cross sections to higher levels were measured for incident neutron energies of 1.2 MeV and above. Since our level scheme does not go beyond 1.17 MeV, and even at this point we are not sure we have accounted for all levels, comparison with experimental results must be interpreted qualitatively. The presence of additional levels will, of course, decrease the calculated values.

The energy captions for the inelastic excitation of a particular level are those given by the experimenter. We therefore used results calculated for the 0.654-MeV level of our level scheme (Fig. 3) to compare with the experimental data labeled as the 0.630$\pm$0.020-MeV

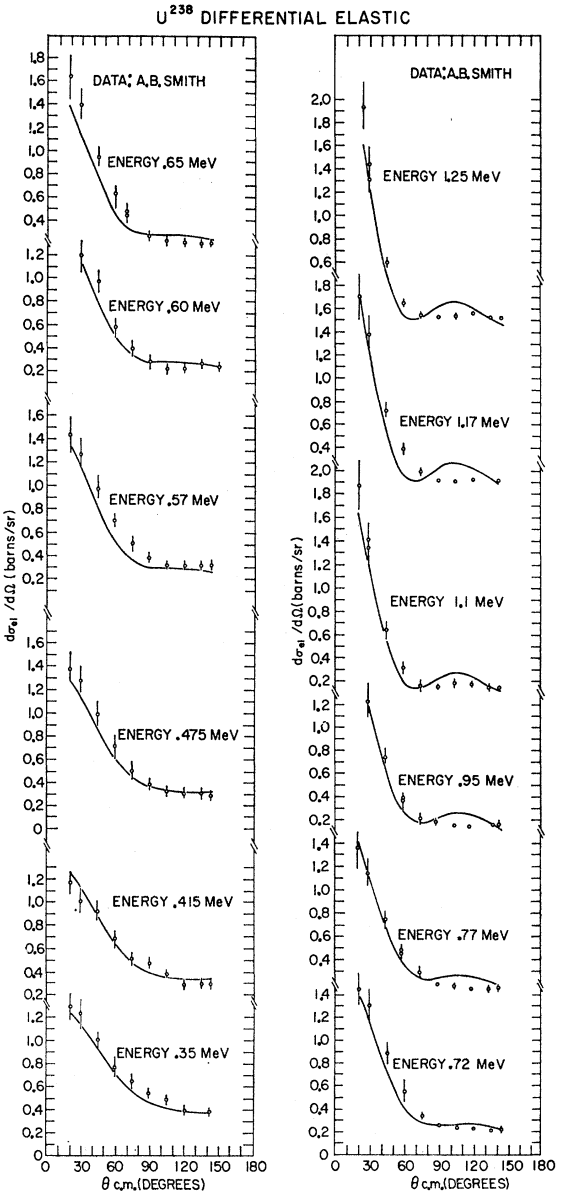

FIG. 5. Experimental and calculated (solid lines) differential elastic scattering cross sections for U for the parameters shown in Fig. 4. Calculated values include corrections for compound elastic scattering using the Hauser-Feshbach theory and the level scheme of Fig. 3.

level in Fig. 2; likewise, calculated results obtained for the 0.710 and 0.728 levels are combined to compare to experimental data at 0.720±0.020 MeV, results for the 0.935-MeV level are compared to data at 0.930±0.030 MeV, and results at 0.986 and 1.03 MeV are combined to compare to data at 1.00±0.03 MeV.

Differential inelastic scattering data[16] for an incident energy of 0.56 MeV for excitation of the first two excited levels are available. The differential cross section for scattering to the first excited level is essentially symmetric about 90° and is fit by the calculated values; for scattering to the second excited level, the calculations predict nearly isotropic results. These are shown in Figure 6.

Th-232

Total neutron cross sections for thorium from 0.1 to 3.0 MeV are taken from BNL-325.[14,20] We assumed

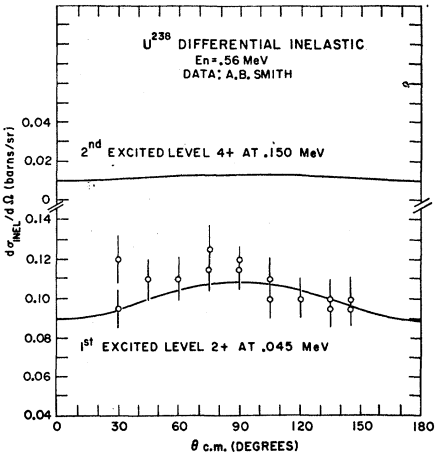

FIG. 6. Differential inelastic-scattering cross sections for the first two excited levels of U^{238}. These correspond to the total inelastic-scattering cross sections of Fig. 2. The experimental data is isotropic for the second excited level.

errors of 10% since the data are over a decade old and are probably not corrected for in-scattering errors.

Differential elastic-scattering cross sections are available at energies: 0.56, 0.70, and 1.00 MeV. These as well as the inelastic-scattering cross sections used are the results of Smith's experiments[21] using pulsed-beam fast time-of-flight techniques. The favorable comparison between this and earlier work, as discussed in Smith's paper, justify using only his results for determining the model parameters.

Two different level schemes were used. One, proposed by Elbek, Igo, Stephens, and Diamond[17] was modified by us to include a 3^+ level at 0.838 MeV; this is shown in Fig. 3. The other level scheme was suggested by Smith[21]

[20] M. Walt, R. L. Becker, A. Okazaki, and R. E. Fields, Phys. Rev. **89**, 1271 (1953).
[21] A. B. Smith, Phys. Rev. **126**, 718 (1962).

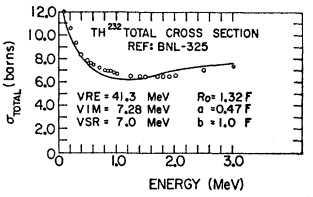

FIG. 7. Experimental and calculated (solid line) values for the neutron total cross section of Th. The data are from Refs. 14 and 20. The calculated values lie within the 10% assigned errors in the data.

and is based on the excitation of residual nuclear levels found experimentally in his inelastic-scattering experiments. We have included some inelastic-scattering calculations with Smith's scheme in Fig. 9 (referred to as level scheme "*b*"). All other calculations, including that of compound elastic corrections, were done with the level scheme of Fig. 3.

The optical-model parameters found as a result of fitting the entrance channel data are: $V_{RE}=41.3$ MeV, $V_{IM}=7.28$ MeV, $V_{SR}=7.0$ MeV, $R_0=1.32$ F, $a=0.47$ F, $b=1.0$ F.

The calculated cross sections using these parameters are compared with the experimental data in Figs. 7 and 8. Agreement is quite good throughout. In Fig. 9, the calculations and data for inelastic scattering are presented. Calculated values for the 6^+ level at 0.330 MeV are small, not exceeding 0.01 b at 1.0 MeV, and are omitted. The results of our calculations are somewhat below the data for the second excited level at 0.170

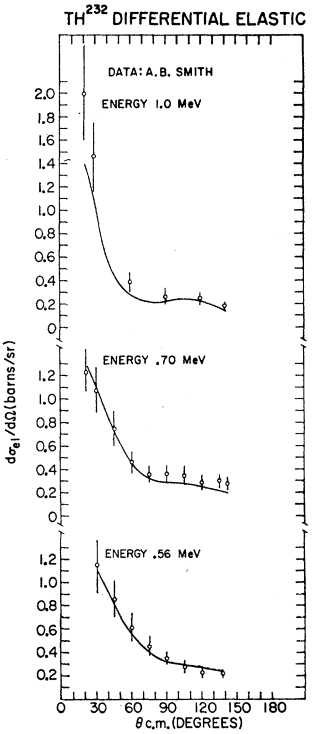

FIG. 8. Differential elastic scattering cross sections for Th. The calculated values (solid lines) are for the parameters of Fig. 7 and include corrections for compound elastic scattering.

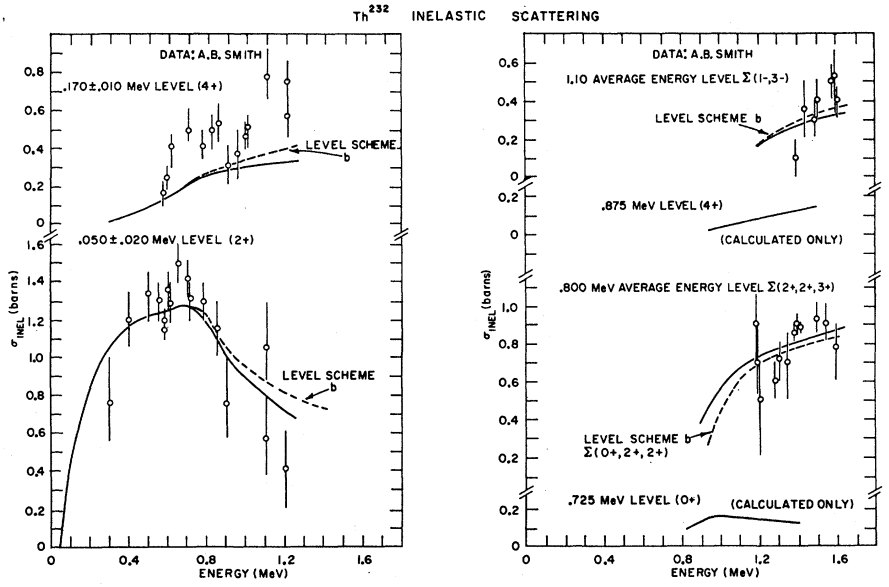

FIG. 9. Cross sections for the inelastic scattering of neutrons by Th^{232}. The calculated values (solid lines) are determined using the Hauser-Feshbach theory and the level scheme of Fig. 3. The dashed lines were calculated using Smith's level scheme (scheme "*b*").

MeV All other levels are fit very well by either level scheme. Since the level scheme does not go beyond 1.2 MeV, calculated values above that energy should be considered only qualitatively. Results below that energy should be correct, assuming no important levels have been missed to that point.

In accord with the previously stated convention, calculated values for the 0.163-MeV level are compared to experimental data at 0.170±0.010 MeV; experimental results at an average energy of 0.800 MeV are compared with the sum of the calculated values for the 0.775-, 0.788-, and 0.838-MeV levels (0.720-, 0.790-, and 0.820-MeV levels for scheme "*b*").

Smith found that differential inelastic cross sections for a neutron of energy 0.56 MeV exciting the first excited level are symmetric about 90°; for excitation of the second excited level, they are isotropic.[21] This is consistent with the Hauser-Feshbach model. Agreement between the calculated values and the data is well within the experimental errors. These are shown in Fig. 10.

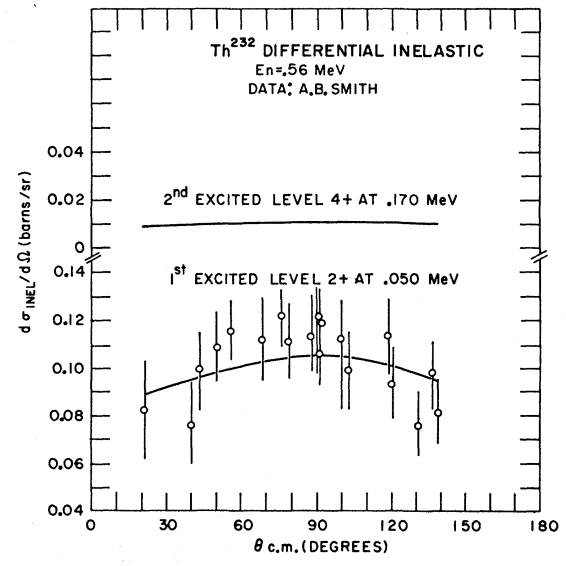

FIG. 10. Differential inelastic scattering cross sections for the first two excited levels of Th^{232}. The calculated values correspond to the solid lines of Fig. 9.

Bi-209

Neutron total cross sections for bismuth from 0.1 to 3.0 MeV are taken from BNL-325[14,22]; the experiments were performed in 1952 and earlier. We assigned an error 10% for fitting purposes. Two sets of angular distribution data[23] were used: one at 0.9 MeV, to which we have assigned errors of 15%, and another at 1.0 MeV, to which errors of 10% are assigned.

The level scheme for bismuth,[24] shown in Fig. 3, is uncomplicated. There are only two excited states below 2.5 MeV.

Kiehn and Goodman[25] measured $(n,n'\gamma)$ cross sections for excitation of the first and second excited states from threshold to 2.8 MeV. Later work,[26] at isolated energy

[22] H. H. Barschall, C. K. Bockelman, and L. W. Seagondollar, Phys. Rev. **73**, 659 (1948); H. H. Barschall, C. K. Bockelman, R. E. Peterson, and R. K. Adair, *ibid.* **76**, 1146 (1949); D. W. Miller, R. K. Adair, C. K. Bockelman, and S. E. Darden, *ibid.* **88**, 83 (1952).

[23] G. N. Lovchikova, At. Energ. (USSR) **2**, 197 (1957); M. Walt and H. H. Barschall, Phys. Rev. **93**, 1062 (1954).

[24] *Nuclear Data Sheets*, compiled by K. Way *et al.* (Printing and Publishing Office, National Academy of Sciences—National Research Council, Washington 25, D. C.).

[25] R. M. Kiehn and C. Goodman, Phys. Rev. **95**, 989 (1954).

[26] L. Cranberg and J. S. Levin, Phys. Rev. **103**, 343 (1956); R. B. Day, *ibid.* **102**, 767 (1956); V. I. Popov, J. Nucl. Energ. **9**, 9 (1959).

points near 2.5 MeV, gives results which indicate that the Kiehn-Goodman data are too large, by almost a factor of 2.

The optical model parameters which fit the entrance channel data and give inelastic-scattering cross sections within the range of the data are: $V_{RE}=46.3$ MeV, $V_{IM}=4.0$ to 2.0 MeV, $V_{SR}=7.0$ MeV, $R_0=1.29$ F, $a=0.50$ F, $b=1.0$ F. The ambiguity in V_{IM} is the result

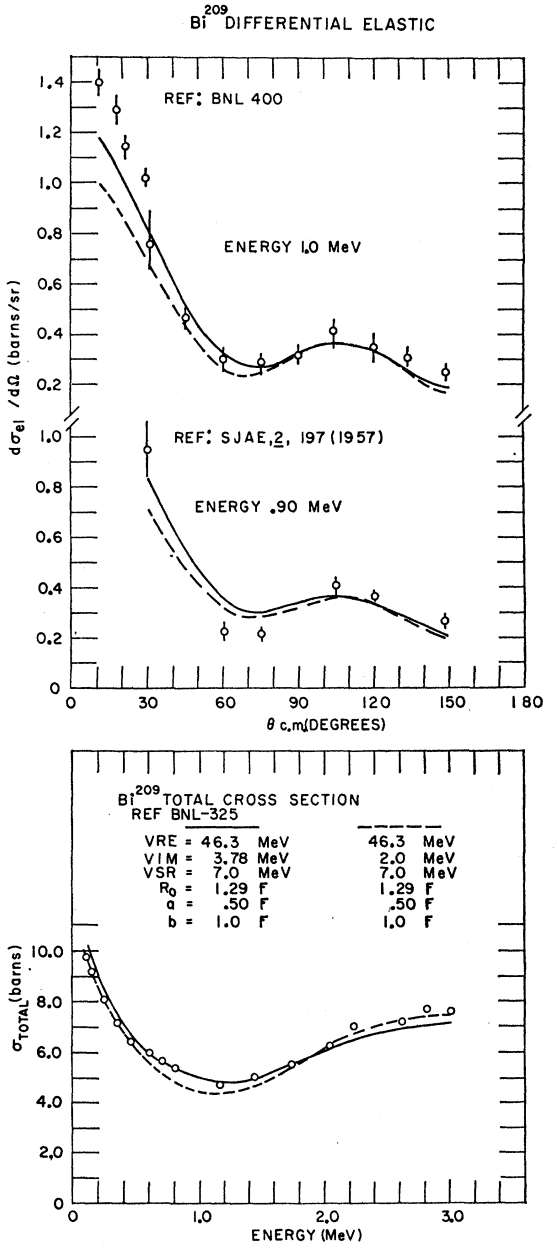

FIG. 11. Neutron total and differential elastic cross sections for Bi. The experimental data are from Refs. 14 and 22. Calculated values of the differential elastic cross sections are corrected for compound elastic contributions. The solid lines are calculated with the parameters stated; the dashed lines are calculated values for the lower limit of V_{IM} (see text).

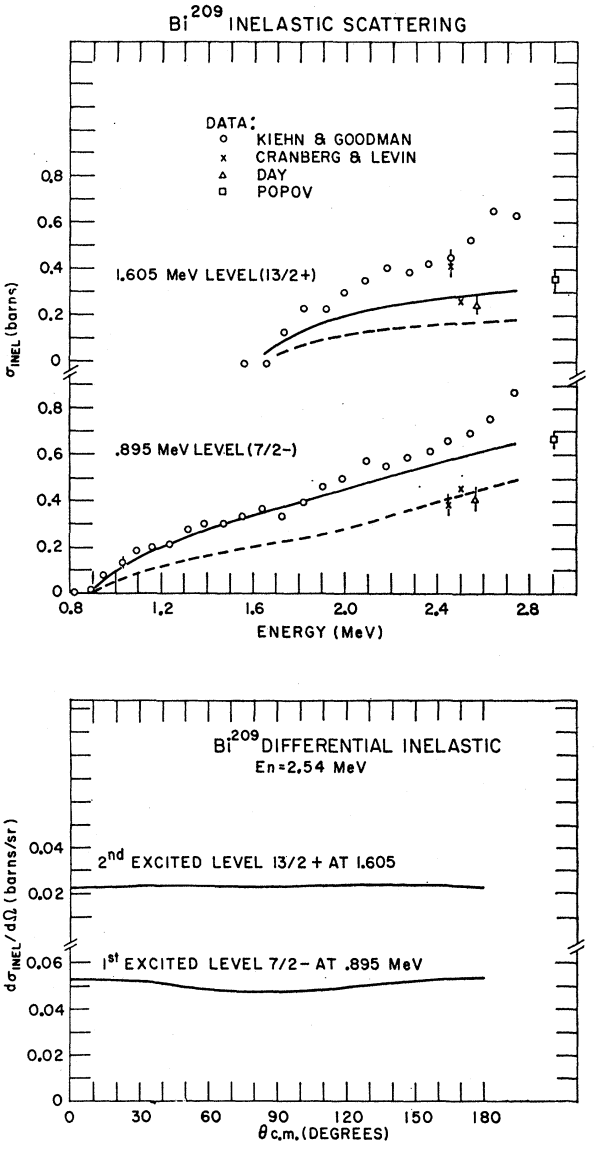

FIG. 12. Cross sections for inelastic scattering of neutrons by Bi^{209}. Calculated values, corresponding to the parameters of Fig. 11, are obtained using the Hauser-Feshbach theory and the level scheme of Fig. 3.

of the entrance channel χ^2 minimum in optical-model parameter space lying along a shallow trough, approximately parallel to the V_{IM} axis. (We have chosen to ignore the trivial variation in other parameters along the principal line of the trough and express the nonuniqueness solely in terms of V_{IM}.) The value $V_{IM}=3.78$ MeV is the low point of this nonsharp minimum region; this value has been used in displaying the results.

The calculated and experimental values for the entrance channel are shown in Fig. 11. Agreement is reasonable. In Fig. 12 the inelastic-scattering cross sections, calculated and experimental, are compared. Kiehn and Goodman's data for the first excited level

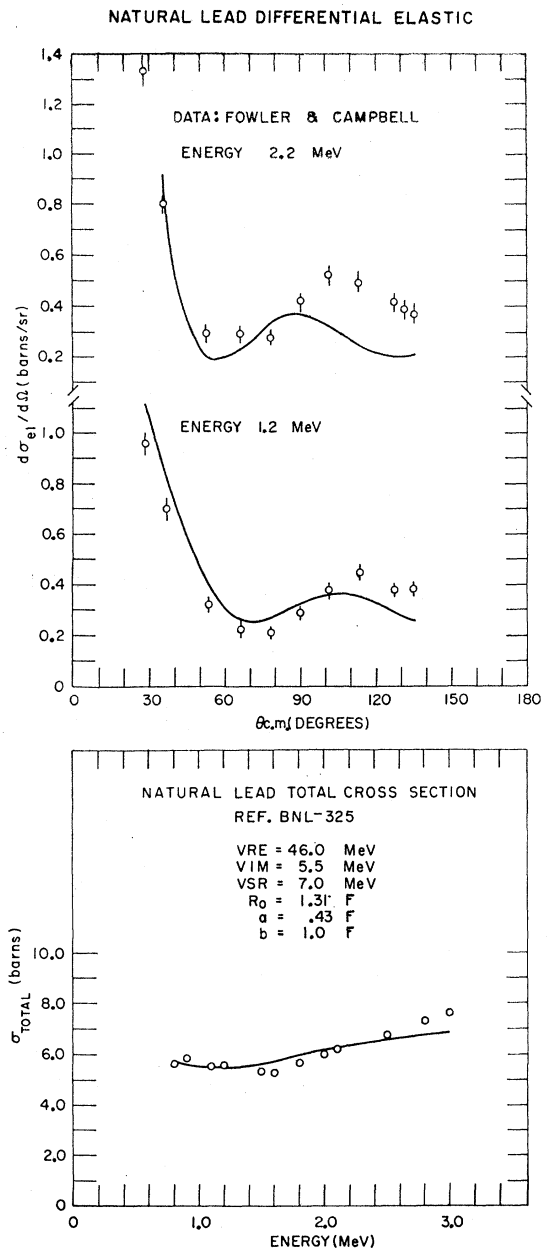

FIG. 13. Total and differential elastic cross sections for scattering neutrons by Pb. The experimental data are from Ref. 14. Calculated values of the differential cross sections are corrected for compound elastic contributions using the level scheme for Pb^{208} alone, as shown in Fig. 3.

favor the set of parameters with larger V_{IM}; their data for the second excited level cannot be fit with any values which fit the entrance channel. The later inelastic-scattering data favor lower values of V_{IM}. Due to the discrepant nature of the data, no definite assignment of parameters is dictated by the inelastic-scattering work. But it is clear that the range of parameters defined by the entrance channel data will contain or be near any final parameters determined by more accurate inelastic scattering data. Figure 12 also shows differential cross sections for inelastic scattering from the first and second excited levels for an incident neutron energy of 2.54 MeV. These agree in shape with recent data of Cranberg.[27]

Pb-208

The neutron total cross section data for lead over the energy range 0.7 to 3.0 MeV is taken from BNL-325.[14] These measurements were made prior to 1952 and lack in-scattering corrections; thus, we assign a 10% error. Total cross sections do exist for isotopically

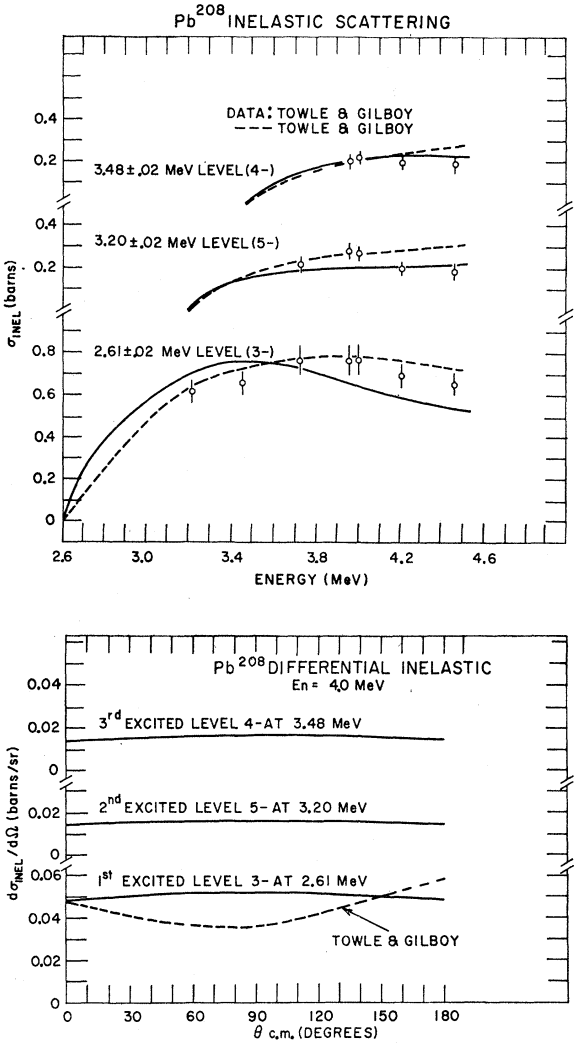

FIG. 14. Cross sections for inelastic scattering of neutrons by Pb^{208}. Calculated values (solid lines), corresponding to the parameters of Fig. 13, are obtained using the Hauser-Feshbach theory with the level scheme of Fig. 3. The calculations of Towle and Gilboy, fitting their inelastic data (Ref. 29) are also shown (dashed lines).

[27] L. Cranberg, J. S. Levin, and C. D. Zafiratos, Bull. Am. Phys. Soc. 8, 82 (1963).

enriched Pb^{208}. The difficulties introduced by the necessity for averaging over resonances and the absence of elastic angular distribution data for isotopic Pb^{208} have made the use of natural lead data more convenient.

Angular distribution data at 1.2 and 2.2 MeV are also for natural lead (51.4% Pb^{208}, 26.7% Pb^{206}, 20.6% Pb^{207}, and 1.3% Pb^{204}). These are from the recent work of Fowler and Campbell[28]; errors given by the authors are used.

The level scheme used for Pb^{208}, shown in Fig. 3, is due to Towle and Gilboy.[29] We also use their inelastic-scattering data and compare our calculations with theirs. There is evidence for the existence of additional levels at 3.99, 4.07, 4.10, 4.20, and 4.23 MeV, but no spins or parities have been assigned them. Since our calculations do not go above 4.4 MeV, the effect of omitting these levels cannot be very large.

One set of optical-model parameters which fit the entrance-channel data for natural lead is: $V_{RE}=46.0$ MeV, $V_{IM}=5.5$ MeV, $V_{SR}=7.0$ MeV, $R_0=1.31$ F, $a=0.43$ F, $b=1.0$ F. There are other sets in this region which fit the data equally well. Note that compound elastic-scattering corrections to the angular distribution data were calculated using the Pb^{208} level scheme while Pb^{208} is only about half the constitution of natural lead. The total cross sections and angular distributions, both calculated and experimental, are compared in Fig. 13. Agreement for total cross sections is reasonable; the 1.2 MeV angular distribution data are fit better than the 2.2-MeV data.

The inelastic-scattering data is for practically pure Pb^{208}. Experimental inelastic-scattering cross sections, together with our calculations using the above parameters are shown in Fig. 14. Comparison with the fitting done by Towle and Gilboy,[29] where only the inelastic-scattering data were used to determine the optical-model parameters, is also shown. The parameters they used included an energy-dependent imaginary well depth; the better fit obtained at higher energies for the first excited level is thus not surprising in view of the additional degree of freedom available. Our agreement, though not as good, did not require energy dependence. Much better agreement would be obtained if the spin of the 3^- level at 3.750 MeV were changed to a much higher value.

The differential cross sections for the inelastic scattering of 4.0-MeV neutrons to the first three excited levels are also shown in Fig. 14. For the first excited level the angular distribution is compared with work done by Towle and Gilboy which is a least-squares fit to their experimental data at an energy of 3.96 MeV. Their results have been normalized to ours at 0° for comparison purposes. There is a pronounced difference in shape between our calculations and their data.

[28] J. L. Fowler and E. C. Campbell, Phys. Rev. 127, 2192 (1962).
[29] J. H. Towle and W. B. Gilboy, Nucl. Phys. 44, 256 (1963).

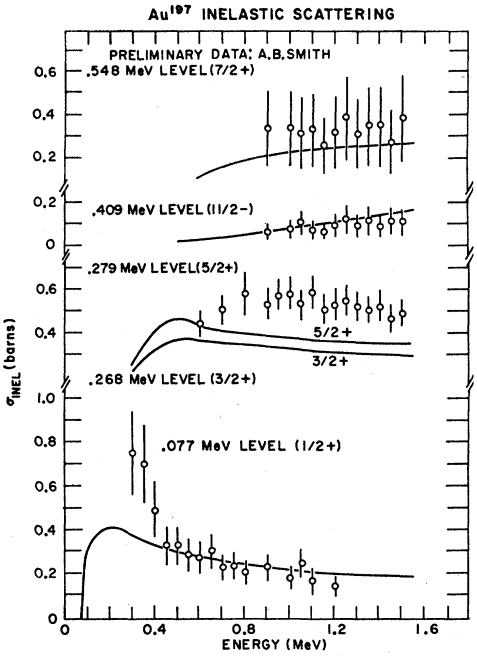

FIG. 15. Cross sections for inelastic scattering of neutrons by Au^{197}. Calculated values are obtained using the Hauser-Feshbach theory and the level scheme of Fig. 16. The data in the second group from the bottom should be compared to the sum of the calculated values for the 0.268-MeV level and the 0.279-MeV level.

Au-197

Total neutron cross sections for gold from 0.1 to 3.0 MeV are from BNL-325.[14,20] As with similar data for other elements, certain corrections have been neglected; thus we assign an error of 10%. Differential elastic scattering cross sections at 0.50, 0.553, 0.59, 0.64, 0.653, 0.69, 0.79, 1.00, 1.10, 1.20, 1.30, and 1.40 MeV as well as the inelastic scattering cross sections are the work of Smith.[30] We have used 10% errors for elastic angular distributions; for the inelastic cross sections the errors assigned by Smith (Fig. 15) were used.

The level scheme used (Figure 16) is taken from the Nuclear Data Tables.[24] Spin and parity assignments are available through 0.548 MeV; the next level is at 1.22 MeV. Comparison with other odd-even nuclei such as $_{79}Au^{195}$, $_{79}Au^{199}$ would support the presence of additional levels between 0.5 and 1.2 MeV. Lind and Day[31] found γ rays of energies 0.474, 0.570, 0.550, 0.670, 0.805, and 0.870 MeV, but the levels from which they originate have not been determined. The results which follow should best be viewed as subject to the possibility that there are missing levels above 0.5 MeV.[32]

[30] A. B. Smith, Bull. Am. Phys. Soc. 9, 461 (1964).
[31] D. A. Lind and R. B. Day, Ann. Phys. (N.Y.) 12, 485 (1961).
[32] After the calculations for this study were performed, we were advised by A. B. Smith that more levels in Au above 540 keV have been found. This seems to bear out our conjectures concerning the origin of some of the discrepancies between our calculations and the data.

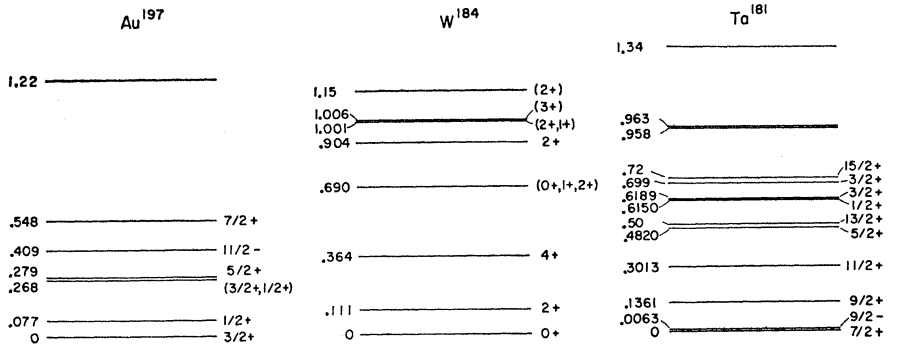

FIG. 16. Level scheme for Au^{197}, W^{184}, and Ta^{181}. These are principally from the *Nuclear Data Tables* (Ref. 24). Spin and parity assignments which are doubtful are given in parentheses with the preferred values first.

We encountered some difficulty in fitting the total and differential elastic cross sections equally well with a single set of parameters. The total cross sections for gold, tungsten, and tantalum were measured in the same experiment. Since questions have been raised concerning the accuracy of the latter two, we stressed the angular distributions over the total cross sections in the final determination of the optical-model parameters. The set adopted is: $V_{RE}=43.2$ MeV, $V_{IM}=4.0$ MeV, $V_{SR}=7.0$ MeV, $R_0=1.31$ F, $a=0.58$ F, $b=1.0$ F.

Values for total cross sections, both calculated and experimental, are shown in Fig. 17. The agreement is poor at lower energies. The elastic angular distributions are shown in Fig. 18. Here agreement is good, except for some of the higher energies. Errors in the compound elastic corrections due to an incomplete level scheme might explain this phenomenon, which apparently sets in at about 0.6 MeV. Furthermore, the experimental angular distributions above 1.00 MeV contain some contributions from the first excited level at 0.077 MeV; this could contribute additional discrepancies.

The inelastic-scattering cross sections for Au^{197} are shown in Fig. 15. We have been unable to fit the bump in the vicinity of 0.2 to 0.3 MeV in the excitation curve for the first excited level with any parameters from the minimum χ^2 region for entrance channel data; thus we have had to content ourselves with agreement for the higher energy part. Smith was unable to distinguish the 0.268-MeV level from that at 0.279 MeV. Accordingly, comparison should be made between the experimental data and the sum of the two calculated curves. Agreement here, as well as for the fourth and fifth excited levels is good.

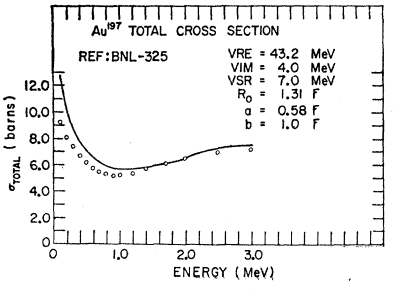

FIG. 17. Neutron total cross sections for Au. The data are from Refs. 14 and 20.

Differential inelastic scattering cross sections for the first three excited levels of Au^{197}, for an incident neutron energy of 0.50 MeV, are shown in Figure 19. These are substantially isotropic for all three levels.

W-184

The total neutron cross sections for natural tungsten are taken from BNL-325.[14,33] Because these experiments

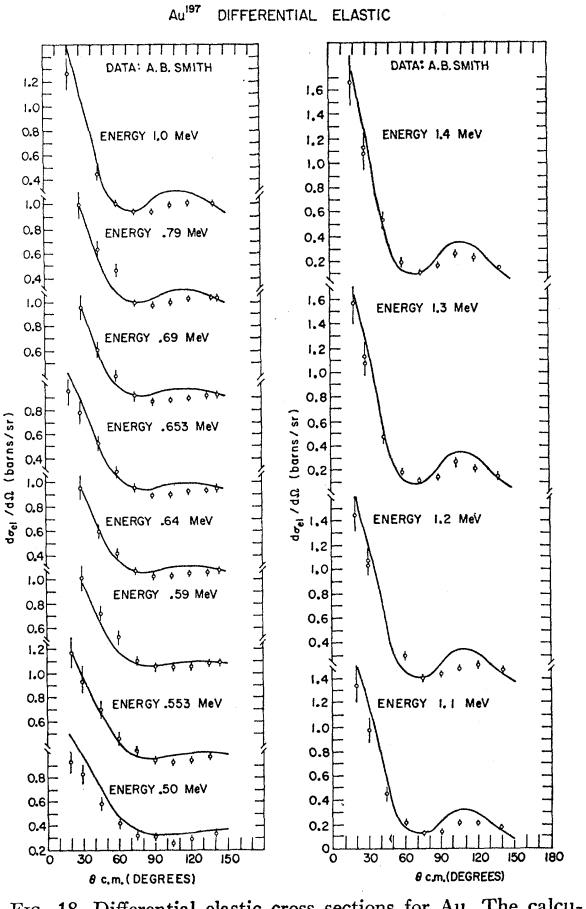

FIG. 18. Differential elastic cross sections for Au. The calculated values (solid lines) correspond to the parameters of Fig. 17 and are corrected for compound elastic-scattering contributions.

[33] R. K. Adair, Phys. Rev. 77, 748 (1950); D. W. Miller, R. K. Adair, C. K. Bockelman, and S. E. Darden, *ibid.* 88, 83 (1952).

are over a decade old, and the experimental technqiues and corrections in analyzing the data are not as refined as today, we assigned errors of 10%. More recent work of Smith[34] indicates that differences exist between the older total data and the totals obtained by summing the elastic and inelastic contributions. Further, he asserts that reactions such as (n,γ) are insufficient to account for the differences. Support is given to his results by other scattering measurements.[35] As a result, we are forced to consider two sets of total cross-section data and examine the consequences of the parameters determined by both.

Differential elastic cross sections for natural tungsten at energies of 0.35, 0.40, 0.475, 0.49, 0.59, 0.64, 0.775, 0.79, 0.95, 1.10, and 1.25 MeV are due to Smith.[34] Natural tungsten consists of 0.14% W^{180}, 26.41% W^{182}, 14.40% W^{183}, 30.64% W^{184}, and 28.41% W^{186}. We have used the level scheme for W^{184} in obtaining the compound elastic-scattering corrections; this raises some questions concerning the calculated elastic-scattering cross sections. However, the strong parallelism between the level structures of W^{180}, W^{182}, W^{184}, and W^{186} should reduce the significance of any errors thereby introduced.

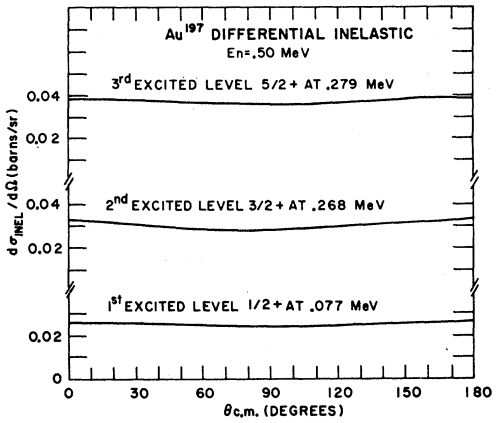

FIG. 19. Neutron differential inelastic-scattering cross sections for the first three excited levels of Au^{197}. These correspond to the total inelastic scattering cross sections of Fig. 15.

The inelastic scattering data, also due to Smith,[34] are for a sample consisting of 1.91% W^{182}, 1.87% W^{183}, 94.3% W^{184}, and 1.91% W^{186}. Because the level scheme for the even-even isotopes are so similar, we treated the experimental data as if they were for 100% W^{184}.

The level scheme for W^{184} is shown in Fig. 16.[24,36] Those spins and parities that are based on systematics and which are questionable are enclosed in parentheses, the first stated ones being preferred.

We found two sets of optical potential parameters:

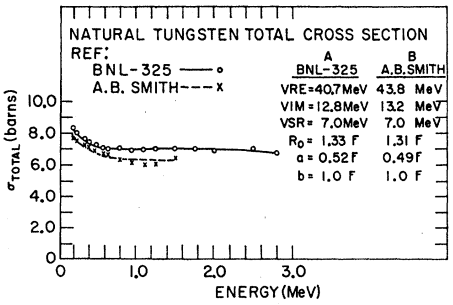

FIG. 20. Neutron total cross sections for W. Two sets of calculated values are shown. Set A (solid line) fits data from Refs. 14 and 33 and Smith's differential elastic data jointly; set B (dashed line) fits Smith's total and differential elastic data jointly.

(A), which satisfies the BNL-325 data and elastic angular distribution data jointly, and (B), which satisfied Smith's total cross sections and elastic angular distribution data jointly.

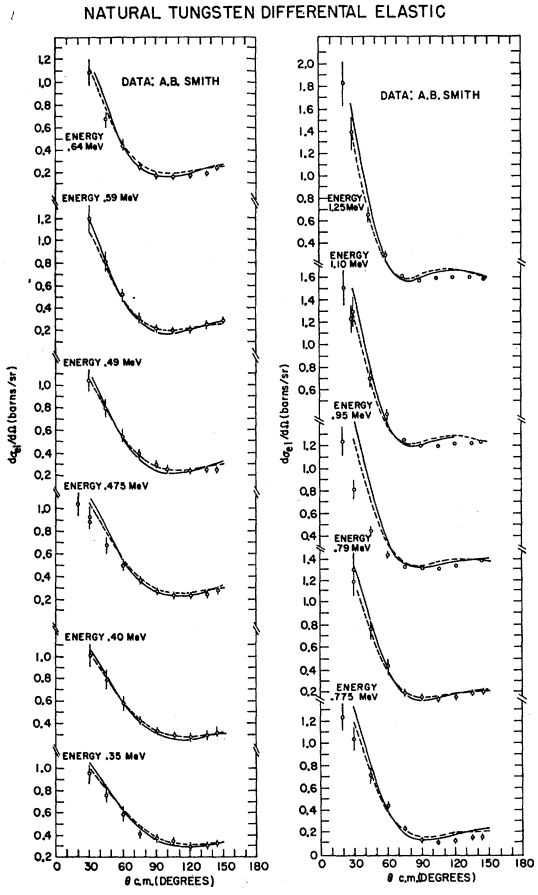

FIG. 21. Differential elastic-scattering cross sections for W. The two sets of calculated values correspond to the parameters of Fig. 20. Only one set of data, those of Smith, are given. Calculated values include corrections for compound elastic scattering using the level scheme of Fig. 16 for W^{184}.

[34] A. B. Smith, Z. Physik **175**, 242 (1963).
[35] A. Langsdorf, R. O. Lane, and J. E. Monohan, Argonne National Laboratory Report ANL-5567, 1961 (unpublished).
[36] N. R. Johnson, Phys. Rev. **129**, 1737 (1963).

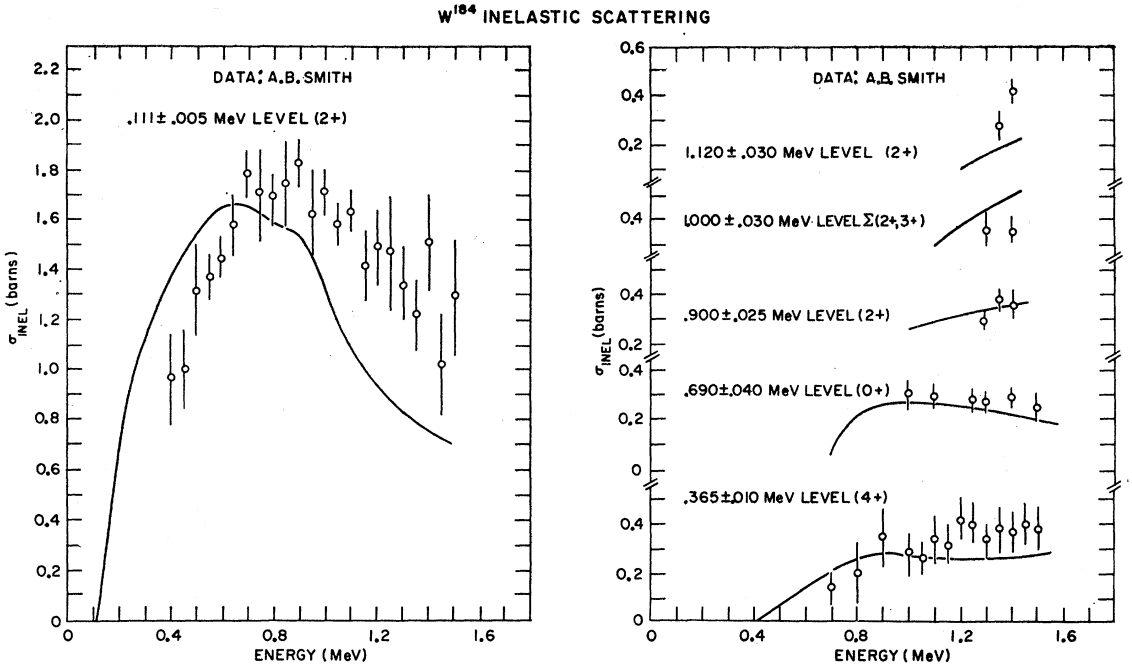

FIG. 22. Cross sections for inelastic scattering of neutrons by W^{184}. Calculated values are for the set A parameters of Fig. 20 using the Hauser-Feshbach theory and the level scheme of Fig. 16.

A	B
$V_{RE}=40.7$ MeV,	$V_{RE}=43.8$ MeV,
$V_{IM}=12.8$ MeV,	$V_{IM}=13.2$ MeV,
$V_{SR}=7.0$ MeV,	$V_{SR}=7.0$ MeV,
$R_0=1.33$ F,	$R_0=1.31$ F,
$a=0.52$ F,	$a=0.49$ F,
$b=1.0$ F,	$b=1.0$ F.

It is notable that there are no radical differences in any of the parameters.

The results for total and differential elastic cross sections are shown in Figs. 20 and 21. Agreement between calculations and the data are quite good for both sets of parameters.

Figures 22 and 23 display the inelastic-scattering cross sections together with the calculated values using parameter set A. The calculated values for all levels above the first excited level are in reasonable agreement with the data. The same is true for calculations with set B. For the first excited level, agreement is poor, though the shape and scale seem good. An energy shift upward of about 0.3 MeV would bring the calculated values into excellent agreement with the data. Set B does not give any better fit to the first excited level; in fact, it gives somewhat lower cross sections while not improving the situation with respect to position on the energy scale.

The differential inelastic cross sections (Fig. 23) are for incident neutrons of 0.50 MeV energy. The first excited level calculated values are symmetric about 90° and about 20% higher than the data which is consistent with the results for total inelastic scattering at that energy; the second excited level is isotropic. The experimental data are isotropic in both cases.

Ta-181

Total neutron cross sections from 0.1 to 3.0 MeV for tantalum are taken from BNL-325.[14,37] As with similarly uncorrected data of the early 1950's, we have assigned errors of 10%. The elastic scattering angular distributions at energies of 0.35, 0.415, 0.47, 0.57, 0.60, 0.65, 0.67, 0.72, 0.77, 0.87, 0.95, 1.02, and 1.10 MeV are the work of Smith,[36] we have assigned 10% errors for fitting purposes. Here, as with tungsten, Smith finds total cross sections which are lower than the BNL-325 data, as much as 1 b in 8 b between 0.3 and 1.4 MeV. This shift is too large to be explained by capture cross sections.

The level scheme, shown in Fig. 16, is from the *Nuclear Data Tables*.[20] We have omitted the level at 0.1588 MeV because its existence is questionable. The inelastic-scattering cross sections are from Smith's work.[38] He finds levels at 0.14±0.01, 0.30±0.01, 0.48 ±0.02, 0.62±0.02, 0.75±0.025, 0.900±0.030, and

[37] C. K. Bockelman, R. E. Peterson, R. K. Adair, and H. H. Barschall, Phys. Rev. **76**, 277 (1949); D. W. Miller, R. K. Adair, C. K. Bockelman, and S. E. Darden, *ibid.* 88, 83 (1952).

[38] A. B. Smith, Argonne National Laboratory Report ANL-6727, 1963 (unpublished).

0.980±0.030 MeV, with indications that the levels at 0.725 and 0.980 MeV consist of two or more components.

The optical potential parameters found in fitting the BNL-325 total cross-section data and Smith's angular distribution data jointly are: $V_{RE}=37.3$ MeV, $V_{IM}=12.1$ MeV, $V_{SR}=7.0$ MeV, $R_0=1.32$ F, $a=0.63$ F, $b=1.0$ F. In Figs. 24 and 25 the calculated cross sections using these parameters (solid lines) are compared with the data. The calculated total cross sections fit

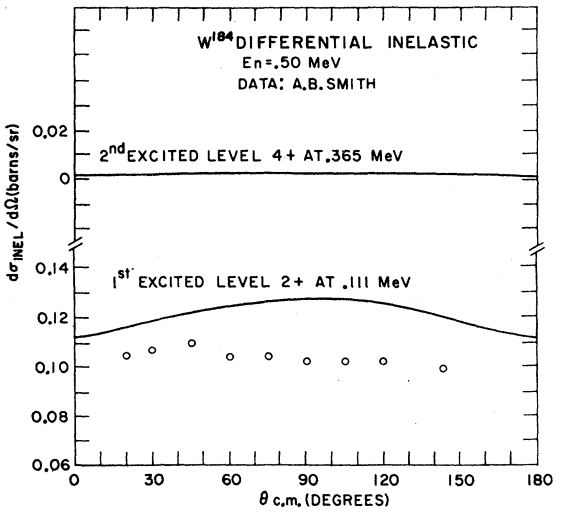

FIG. 23. Neutron differential inelatic-scattering cross sections for the first two excited levels of W^{184}. These correspond to the total inelastic-scattering cross sections of Fig. 22.

the experimental data well; agreement for the angular distributions is only fair.

Figures 26 and 27 display the calculated and experimental values of the inelastic-scattering cross sections for the levels up to 0.725 MeV and of the differential inelastic scattering cross sections for an incident neutron energy of 0.710 MeV for the second and third excited levels. Agreement for the total inelastic cross sections is quite good.

Since our level scheme does not have spin assign-

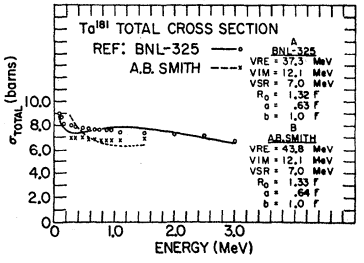

FIG. 24. Neutron total cross sections for Ta. The values calculated using the parameters of set A (solid line) fit the data from Refs. 14 and 37 and Smith's differential elastic data jointly.

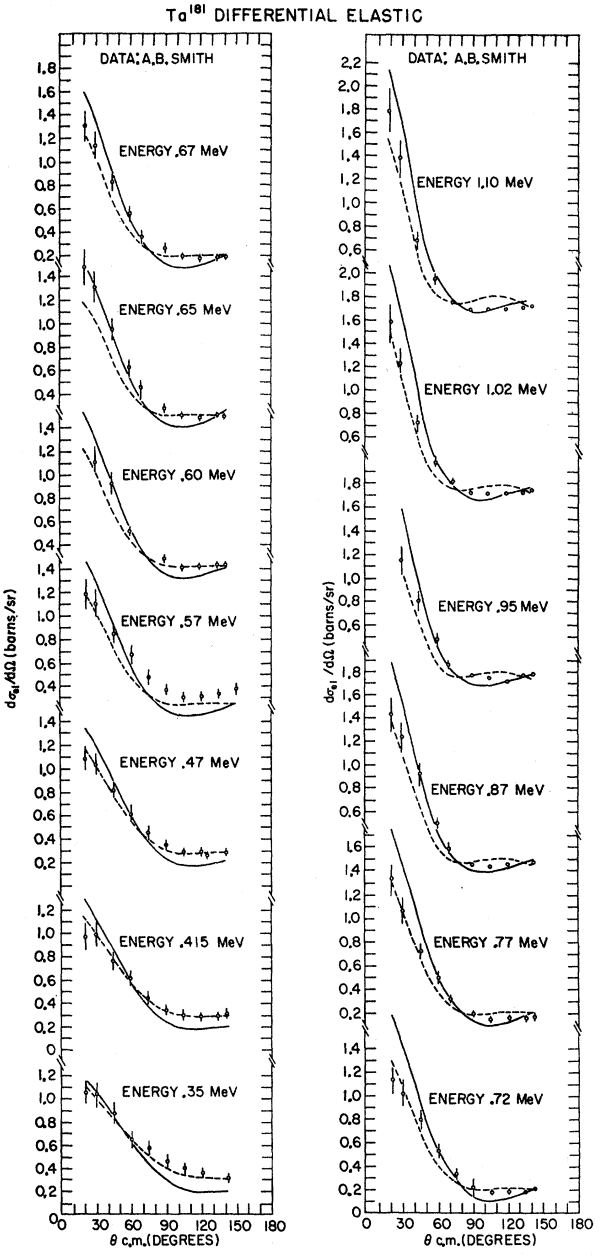

FIG. 25. Differential elastic-scattering cross sections for Ta. The two sets of calculared values correspond to the parameters of Fig. 24 and include corrections for compound elastic scattering.

ments for levels above 0.720 MeV and additional levels do exist in the range 0.9 to 1.0 MeV, the inelastic-scattering cross sections should be depressed somewhat above 1.0 MeV. In Fig. 27 we have also included a comparison with the angular distribution data of Rogers, Garber, and Shrader[39]; their results show some struc-

[39] W. L. Rogers, D. I. Garber, and E. F. Shrader, Bull. Am. Phys. Soc. 6, 61 (1961); also, E. F. Shrader (private communication).

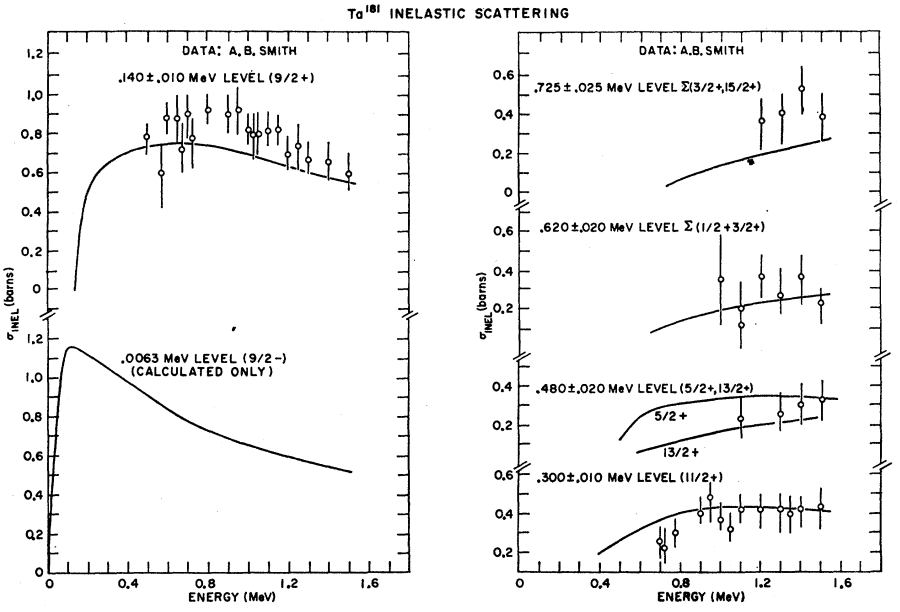

FIG. 26. Cross sections for inelastic scattering of neutrons by Ta^{181}. Calculated values are for the set A parameters of Fig. 24 using the Hauser-Feshbach theory and the level schemes of Fig. 16. No data are available for the first excited level.

ture. The calculations agree with Smith's data, which are isotropic.

On seeking parameters which fit both Smith's total cross sections and elastic angular distributions jointly, the best we could do on a not too intensive search beginning from the parameters of set B for W^{184}, was to obtain agreement in total cross sections only above 0.6 MeV while improving the angular distributions considerably (dashed lines, Figs. 24 and 25). The over-all fitting is thus poorer than above. The inelastic-scattering calculations (not shown) with these parameters are not as good as for the primary set of parameters. The nature of the data is such that further attempts to reconcile calculations with experiment do not seem warranted at this time.

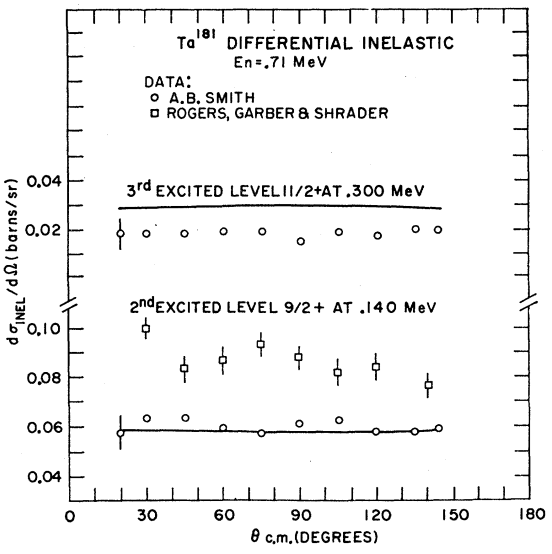

FIG. 27. Neutron differential inelastic-scattering cross sections for the second and third excited levels of Ta^{181}. These correspond to the total inelastic-scattering cross sections of Fig. 26.

IV. DISCUSSION

The entrance-channel data have been fit reasonably well using the rather simple optical model outlined in Sec. II, with parameters determined separately for each element. The inclusion of a spin-orbit interaction term in the potential is necessary, though the final value of V_{SR} as a result of any particular search is subject to large uncertainties. (We would caution against drawing any conclusions from the rather large value of V_{SR} found for uranium.)

In two of the cases, Pb and W, where the compound elastic corrections to differential elastic scattering were calculated using the level schemes for a single isotope while the data were for the natural element, agreement is not as good as elsewhere. A more refined calculation, using averages over isotope mixtures, might well have produced better parameters. However, we would not expect them to be sufficiently different to invalidate the inelastic scattering calculations completely.

Further, in those cases where some levels have been missed, the compound elastic corrections, as computed, are too large. This is probably the case with Au above 0.6 MeV.[32]

No necessity has been found for additional parameters such as different radii for the real and imaginary parts of the optical potential, or the addition of a volume component to the imaginary part, etc. The analysis

presented here does not prejudice any theoretical motivation for additional parameters. Rather, within the terms of a phenomenological study, we find that the data do not *require* additional parameters of this nature. The free parameters included appear to be sufficient to "cover up" any such effects, if they are indeed present.

On the whole, the energy-independent parameters obtained for the entrance channel data give good enough agreement to warrant testing them against the inelastic data.

Calculations for inelastic-scattering cross sections are dependent upon the level schemes used. In the case where there are many levels, the results are not too sensitive to the details of the level scheme in that minor changes in spin and parity assignments or slight shifts in energies do not appreciably change the cross-section values. We have used the best available estimates for the level schemes. In some areas, such as Au^{197} or Ta^{181}, incompleteness in the level schemes can affect the results.[32] These have been noted in the detailed discussions above.

Much consideration has been given to the relation between the transmission coefficients T and the elements of the scattering matrix η. We have used the simple relation exclusively. Though some modification of the calculated values would result from the use of correction terms,[9] the errors in the data and the general features of the inelastic-scattering calculation here presented do not appear to warrant inclusion of such details. Perhaps, when much more accurate data, particularly in the vicinity of threshold, is available a reexamination of this point will be justified. If viewed with such considerations in mind, the 4^+ levels in U^{238} and Th^{232} might be construed to show thresholds effects. However, the mass of data does not seem to demand this construction.

We did not include effects due to deformation or width distributions. U^{238} and Th^{232} are highly deformed; yet good agreement between calculations and experiment were obtained. Chase, Wilets, and Edmonds[40] considered the contributions due to direct rotational excitation of U^{238} and found a small (compared to compound nucleus) contribution from this source. The most significant effect would appear in the angular distribution. In our Fig. 6, however, the data are fit well within the experimental errors by the Hauser-Feshbach model. Ta^{181} and W^{184}, also deformed nuclei, were not fit as well, though the general features of the inelastic cross sections were reproduced. Here, the data was not as good as for U or Th. Dresner[41] has considered the effects of width distributions and found that, in certain cases, the effect upon the cross section could be quite large. It appears from our study that a spherical optical potential can yield equivalent parameters which "cover up" these effects.

Finally, any related elements, i.e., U^{238} and Th^{232}, Bi^{209}, and Pb^{208}, etc., have similar parameters. We also find that the strength of the imaginary part of the potential is related to the distance from closed shells. Pb and Bi have small absorption as contrasted to the others.

V. CONCLUSIONS

The fitting of entrance-channel data for heavy nuclei with a spherical, local, spin-dependent optical potential (including corrections for compound elastic scattering) gives parameters which reproduce neutron-scattering data quite well. When coupled with the Hauser-Feshbach theory for inelastic scattering and a reasonable set of level assignments, they give calculated cross sections for inelastic scattering which adequately fit the general features of the experimental data. The latitude allowed by the nonsharp minima in the optical-model parameter space provides the ability to fit both entrance channel and inelastic-scattering data with a relatively simple model. Further refinements depend on the accuracy of the data. The effects of deformation, width distributions and variation of parameters with energy should be considered as the data are improved; some indications of these may already be present in the 4^+ levels of Th^{232} and U^{238}.

Tabulated values of differential elastic cross sections for many of the elements of this paper have been issued.[42]

ACKNOWLEDGMENTS

We should like to thank Dr. Alan B. Smith for allowing us the use of his data prior to publication. We would also like to thank Dr. C. E. Porter for valuable discussions. The cooperation of the staff of the BNL Computer Center, whose IBM-7090/94 was used for the calculations, made the massive computation job tolerable. The assistance of Miss Frances Pope, who maintained records, plotted preliminary data, and otherwise kept the considerable quantity of data and computational results manageable, is most gratefully acknowledged.

[40] D. M. Chase, L. Wilets, and A. R. Edmonds, Phys. Rev. **110**, 1080, (1958).

[41] L. Dresner, Proceedings of the International Conference on Neutron Interactions with Nuclei, Columbia University, 1957 [Atomic Energy Commission Report TID-7547 (unpublished)]; also see A. M. Lane and J. E. Lynn, Proc. Phys. Soc. (London) **A70**, 557 (1957).

[42] S. O. Moore and E. H. Auerbach, Brookhaven National Laboratory Report, BNL-818, 1963 (unpublished).